

1 Transplantation of high fat fed mouse microbiota into zebrafish larvae identifies MyD88-  
2 dependent acceleration of hyperlipidaemia by Gram positive cell wall components

3

4 Pradeep Manuneedhi Cholan<sup>1</sup>, Simone Morris<sup>1</sup>, Kaiming Luo<sup>1</sup>, Jinbiao Chen<sup>2</sup>, Jade A Boland<sup>2</sup>, Geoff  
5 W McCaughan<sup>2,3</sup>, Warwick J Britton<sup>1,4</sup>, Stefan H Oehlers<sup>1,5</sup> \*

6 <sup>1</sup> Tuberculosis Research Program at the Centenary Institute, The University of Sydney,  
7 Camperdown, NSW 2050, Australia

8 <sup>2</sup> Liver Injury and Cancer Program at the Centenary Institute, The University of Sydney,  
9 Camperdown, NSW 2050, Australia

10 <sup>3</sup> AW Morrow Gastroenterology and Liver Centre, Royal Prince Alfred Hospital, Camperdown, NSW  
11 2050, Australia

12 <sup>4</sup> Department of Clinical Immunology, Royal Prince Alfred Hospital, Camperdown, NSW 2050,  
13 Australia

14 <sup>5</sup> The University of Sydney, Discipline of Infectious Diseases & Immunology and Marie Bashir  
15 Institute, Camperdown, NSW 2050, Australia

16

17

18 Corresponding author: Dr Stefan Oehlers [s.oehlers@centenary.org.au](mailto:s.oehlers@centenary.org.au)

19 ORCID: 0000-0003-0260-672X Twitter: @oehlerslab

20

21 Keywords: zebrafish, hyperlipidaemia, microbiota, pathobiont, myd88

22

### 23 **Abstract**

24 Gut dysbiosis is an important modifier of pathologies including cardiovascular disease but our  
25 understanding of the role of individual microbes is limited. Here, we have used transplantation of

26 mouse microbiota into microbiota-deficient zebrafish larvae to study the interaction between  
27 members of a mammalian high fat diet-associated gut microbiota with a lipid rich diet challenge in  
28 a tractable model species. We find zebrafish larvae are more susceptible to hyperlipidaemia when  
29 exposed to the mouse high fat-diet-associated microbiota and that this effect can be driven by  
30 two individual bacterial species fractionated from the mouse high fat-diet-associated microbiota.  
31 We find *Stenotrophomonas maltophilia* increases the hyperlipidaemic potential of chicken egg  
32 yolk to zebrafish larvae independent of direct interaction between *S. maltophilia* and the zebrafish  
33 host. Colonisation by live, or exposure to heat-killed, *Enterococcus faecalis* accelerates  
34 hyperlipidaemia via host Myd88 signalling. The hyperlipidaemic effect is replicated by exposure to  
35 the Gram positive Toll-like receptor agonists peptidoglycan and lipoteichoic acid in a MyD88-  
36 dependent manner. In this work, we demonstrate the applicability of zebrafish as a tractable host  
37 for the identification of gut microbes that can induce conditional host phenotypes via microbiota  
38 transplantation and subsequent challenge with a high fat diet.

39

#### 40 **Introduction**

41 The metagenome encoded by the gut microbiome is an essential component of the animal  
42 digestive system [1, 2]. Microbes can affect digestion directly through the breakdown of  
43 indigestible material such as fibre to short chain fatty acids and indirectly by stimulating the  
44 differentiation of the intestinal epithelium.

45

46 The microbiome is shaped by host and environment selective pressures [3, 4]. Lipid-rich Western  
47 diets that cause obesity in susceptible individuals are associated with gut dysbiosis which can drive  
48 an unwanted increase in nutrient absorption and epithelial leakiness [5]. Transplantation of  
49 human lean and obese microbiota into germ-free mice transmits these phenotypes across host-  
50 mammalian species [6]. While the germ-free mouse has been invaluable for the study of host-

51 microbe interactions through gnotobiotic and transplantation studies, there is a need for faster  
52 and more accessible models that serve as functional screening tools for disease-associated  
53 microbiota.

54

55 Zebrafish embryos require microbial colonisation during development for full physiological  
56 digestive function and are a simple platform for studying host-microbiota-environment  
57 interactions [7, 8]. Zebrafish embryos develop *ex utero* within a chorion that can be surface  
58 sterilised and are tolerant of antibiotics in their media making them a technically simple model for  
59 raising germ-free experimental subjects. Probiotic transfer has been shown to increase resistance  
60 to pathogen colonisation [9]. The zebrafish gut microbiome is sensitive to challenge with a HFD,  
61 feeding larval zebrafish a diet supplemented with 10% fat for 25 days altered the distribution of  
62 bacterial phyla in the gut which correlated with increased expression of host inflammatory genes  
63 compared to larvae fed the control diet [3].

64

65 Microbiota transplants have been previously performed from mice and humans to zebrafish  
66 demonstrating the feasibility of using the zebrafish as an *in vivo* screening tool for studying the  
67 effects of defined microbiota on host physiology [10]. Here we use this technically simple model to  
68 rapidly identify specific members of the mouse HFD-associated microbiota that accelerate a diet-  
69 induced hyperlipidaemic phenotype in zebrafish embryos and the mechanisms by which these  
70 pathogens interact with the zebrafish host.

71

## 72 **Results**

73 Transplantation of microbiota from HFD fed mice accelerates hyperlipidaemia in zebrafish  
74 embryos

75 Microbiome-depleted (MD) zebrafish embryos were exposed to mouse faecal microbiota  
76 preparations generated from mice fed a conventional chow diet or HFD from 3-5 dpf (days post  
77 fertilization) and challenged with chicken egg yolk feeding from 5-7 dpf (Figure 1A).

78

79 We first investigated if colonisation with the control or HFD-fed mouse microbiota affected  
80 zebrafish intestinal physiology at 5 dpf before the onset of exogenous feeding. The absorptive  
81 activity of zebrafish midgut lysosome-rich intestinal epithelial cells can be visualised by neutral red  
82 staining, previous studies have demonstrated that this phenotype requires microbial colonisation  
83 and is impeded by inflammation [11, 12]. We used neutral red staining visually to examine the  
84 absorptive function of colonised embryos and observed higher staining in 5 dpf larvae colonised  
85 with the HFD-fed microbiota compared to chow diet colonised controls (Figure 1B and 1C).

86

87 We next collected colonised zebrafish larvae and stained with Oil Red O to visualise neutral lipids  
88 but did not observe any differences in lipid staining. To determine if colonisation with the HFD-fed  
89 mouse microbiota affected the zebrafish response to challenge with a chicken egg yolk challenge  
90 [13], we challenged 5 dpf zebrafish with chicken egg yolk and stained with Oil Red O to visualise  
91 neutral lipids (Figure 1D). Zebrafish larvae colonised with the faecal microbiota from HFD fed mice  
92 had more vascular Oil Red O staining after 2 day of chicken egg yolk feeding challenge compared  
93 to zebrafish larvae colonised with the faecal microbiota from chow diet fed mice (Figure 1E).

94

95 These data demonstrate the responsiveness of MD zebrafish larvae to the transferable effects of  
96 dysbiotic mammalian gut microbiome-associated microbiota when challenged with a complex  
97 environmental stimulus in the form of lipid-rich feeding.

98

99 Identification of individual microbes with pathobiont activity

100 To isolate individual species that would be amenable to *in vitro* handling and growth, faecal  
101 homogenate supernatants were plated on LB agar and grown at 28°C to select for species that  
102 would be easily handled and most likely to colonise zebrafish embryos (Figure 2A). The best  
103 growing isolate in LB broth culture from two chow diet and HFD fed faecal preparations were  
104 selected and sequenced. We identified *Enterococcus faecalis* strain YN771 (*E.f* on figures) and  
105 *Stenotrophomonas maltophilia* strain CD103 (*S.m*) from HFD-fed mouse faecal lysate, and  
106 *Escherichia* species PYCC8248 (*E.s*) and *Escherichia coli* strain Y15-3 (*E.c*) from chow diet-fed  
107 mouse faecal lysate.

108

109 We colonised MD zebrafish larvae with individual isolates to determine if monoassociation could  
110 replicate the effects of bulk microbiota transfer. To determine if exposure of larvae to  
111 preparations of *E. faecalis*, *S. maltophilia*, or either of the *E. coli* strains resulted in gut colonisation  
112 we dissected guts from rinsed 5 dpf larvae after 2 days of monoassociation exposure and  
113 recovered bacteria onto LB agar. All tested strains yielded recoverable colonisation levels of  
114 approximately 100 CFU per larval gut. Gnotobiotic zebrafish larvae colonised with *E. faecalis* or *S.*  
115 *maltophilia* had increased Oil Red O staining compared to larvae colonised with either of the  
116 *Escherichia* strains after chicken egg yolk challenge (Figure 2B).

117

118 Interestingly, colonisation with *E. faecalis* or *S. maltophilia* did not increase the absorptive activity  
119 of the midgut intestinal epithelium compared to larvae colonised with either of the *Escherichia*  
120 strains suggesting the absorptive phenotype seen in bulk microbiota transplant is the product of  
121 multiple microorganisms or metabolites present in the complex mouse faecal microbiota  
122 preparations (Figure 2C).

123

124 We next sought to confirm our observations using a second strain of each bacterial species, *E.*  
125 *faecalis* UNSW 054400 type strain (*E.f* UNSW) and *S. maltophilia* yy01 (*S.m* yy01) isolated from  
126 another mouse in the same facility. Colonisation of MD zebrafish embryos with either strain  
127 replicated the hyperlipidaemic phenotype seen with our original isolates (Figure 2D). Interestingly,  
128 the type UNSW 054400 strain increased hyperlipidaemia beyond that seen with our YN771 isolate  
129 strain, while conversely the *S. maltophilia* yy01 strain was not as potent as our original CD103  
130 strain, demonstrating strain-specific variability in our zebrafish embryo system.

131

132 *Stenotrophomonas maltophilia* can accelerate hyperlipidaemia by digesting food external to the  
133 host

134 To identify the mechanisms by which *E. faecalis* and *S. maltophilia* were accelerating HFD-induced  
135 hyperlipidaemia in zebrafish larvae, we sought to investigate if the bacteria needed to be alive  
136 and/or in contact with the host.

137

138 We adapted our gnotobiotic methodology to expose MD embryos to heat killed bacterial  
139 preparations prior to chicken egg yolk feeding (Figure 3A). Exposure to heat-killed *E. faecalis*  
140 replicated the live *E. faecalis* hyperlipidaemic phenotype when compared MD embryos that had  
141 been exposed to either heat killed *S. maltophilia* or either of the *Escherichia* strains (Figure 3B).  
142 Conversely, heat-killed *S. maltophilia* did not induce hyperlipidaemia in concert with chicken egg  
143 yolk challenge.

144

145 We hypothesised *S. maltophilia* might interact with the chicken egg yolk independently of the host  
146 colonisation. To test this hypothesis, we incubated chicken egg yolk with each of our 4 bacterial  
147 isolates in conditions representative of the zebrafish embryo media and then sterilised the “pre-  
148 digested” chicken egg yolk by autoclaving prior to feeding to MD zebrafish embryos (Figure 3C).

149 Compared to either untreated chicken egg yolk, autoclaved chicken egg yolk, or chicken egg yolk  
150 incubated with the other three bacterial isolates, the chicken egg yolk that had been incubated  
151 with *S. maltophilia* increased hyperlipidaemia in zebrafish embryos (Figure 3D). A weaker, but  
152 statistically significant, effect was also seen with chicken egg yolk that had been incubated with  
153 *Escherichia coli* strain Y15-3 (*E.c.*).

154

155 We next repeated this experiment in conventionally raised embryos and found the increased  
156 hyperlipidaemic potential of *S. maltophilia* “pre-digested” chicken egg yolk was replicated in  
157 larvae with a conventional microbiome (Figure 3E).

158

159 To examine the substrate specificity of *S. maltophilia*, we incubated commercially available fish  
160 embryo food with *Escherichia coli* strain Y15-3 or *S. maltophilia* and observed an increase in body  
161 size of only in embryos fed the commercial feed that had been “pre-digested” with *S. maltophilia*  
162 compared to untreated commercial feed (Figure 3F).

163

164 Visual inspection of *S. maltophilia* “pre-digested” chicken egg yolk suspensions suggested *S.*  
165 *maltophilia* had broken apart the chicken egg yolk resulting in smaller particles that could be more  
166 easily ingested and altered the biochemical properties of the chicken egg yolk as the solution  
167 contained much finer particles than for other treatments (Figure 3G). An intermediate phenotype  
168 was seen in chicken egg yolk that had been “pre-digested” by *E. coli* strain Y15-3. CFU recovery  
169 assays demonstrated higher growth of *S. maltophilia* than *E. coli* strain Y15-3 suggesting the better  
170 growth of *S. maltophilia* may convert chicken egg yolk into components that could be digested by  
171 zebrafish embryos (Figure 3H). We performed nutritional panel and free fatty acid analyses of  
172 chicken egg yolk that had been “pre-digested” by *S. maltophilia* or *E. coli* strain Y15-3 as an  
173 additional control (Table 1). These analyses revealed only a modest increase in energy content by

174 *E. coli* strain Y15-3 and *S. maltophilia*, and an increase in total fat content made up of  
175 monounsaturated and saturated fatty acids in *S. maltophilia*-incubated samples that was not seen  
176 in control or *E. coli* strain Y15-3-incubated samples.

177

178 These data illustrate a colonisation-independent mechanism by which *S. maltophilia* may enhance  
179 lipid uptake in zebrafish larvae by modifying food in the aqueous environment external to the  
180 host.

181

182 *Enterococcus faecalis* accelerates hyperlipidaemia via host MyD88-mediated signalling

183 Our analyses had shown *E. faecalis* did not need to be alive but did need to be pre-associated with  
184 the hatching zebrafish larvae to accelerate hyperlipidaemia suggesting colonisation of the gut or  
185 other mucosal surfaces and subsequent recognition by the host may have been necessary to accelerate  
186 hyperlipidaemia. Host innate immune signalling via the Myd88 adaptor protein is essential for the  
187 zebrafish intestinal epithelium to respond to microbial colonisation [14].

188

189 We performed knockdown of host *myd88* expression using multiple CRISPR-Cas9 gRNAs (Figure  
190 4A). Host *myd88* expression was necessary for transducing the *E. faecalis*-induced hyperlipidaemic  
191 signal as *myd88* crisprants had significantly less vascular Oil Red O staining than scrambled  
192 gRNA/Cas9-injected control embryos after colonisation with *E. faecalis* and chicken egg yolk  
193 challenge (Figure 4B).

194

195 Gram positive cell wall components accelerate hyperlipidaemia in zebrafish embryos

196 *E. faecalis* is a Gram-positive bacterium. To determine if *E. faecalis*-driven hyperlipidaemia was  
197 due to a conserved Gram-positive cell wall component, we initially compared the hyperlipidaemic  
198 potential of heat-killed *E. faecalis* to heat killed *Staphylococcus xylosus* (*S.x*), another Gram-

199 positive bacterium obtained from the faecal microbiota of a mouse from the same facility. We  
200 found exposure of zebrafish larvae to heat-killed *S. xylosus* replicated the hyperlipidaemic effect of  
201 heat-killed *E. faecalis* after chicken egg yolk challenge (Figure 5A).

202

203 Next we directly soaked MD larvae in a sublethal dose of 25 µg/mL purified lipoteichoic acid (LTA)  
204 or peptidoglycan (PGL), which are major components of the Gram-positive cell wall, prior to  
205 challenge with chicken egg yolk feeding [15]. Either one of these purified ligands were able to  
206 accelerate hyperlipidaemia in MD larvae (Figure 5B).

207

208 To test the requirement for intact *E. faecalis* PGL to accelerate hyperlipidaemia, we exposed MD  
209 larvae to lysozyme-digested heat-killed *E. faecalis* prior to chicken egg yolk feeding. Lysozyme  
210 digestion ablated the ability of heat-killed *E. faecalis* to accelerate hyperlipidaemia (Figure 5C).

211

212 To determine if host innate immune signalling via the Myd88 adaptor protein transduced the LTA  
213 or PGL-induced signal that accelerates hyperlipidaemia, we again knocked down *myd88* using a  
214 pooled CRISPR-Cas9 gRNA approach and exposed crisprants to LTA or PGL. Depletion of host *myd88*  
215 ablated the sensitivity of embryos to LTA and PGL-induced accelerated hyperlipidaemia (Figure  
216 5D).

217

218 Together, these experiments demonstrate larval zebrafish lipid metabolism is sensitive to the  
219 presence of Gram-positive bacterial cell wall components via Myd88-mediated host signalling  
220 pathways.

221

222 **Discussion**

223 Our study demonstrates the utility of the gnotobiotic zebrafish platform to screen donor  
224 microbiota samples for transplantable biological activities in combination with an exogenous  
225 environmental factor. The addition of an exogenous trigger to the experimental system is an  
226 important permutation that allows the identification of microbes whose interactions with the host  
227 only become apparent in combination with an environmental challenge such as diet.

228

229 We applied the gnotobiotic zebrafish platform to explore the diet-hyperlipidaemia axis as there is  
230 a growing interest in microbiome studies within the cardiovascular disease field [16]. The  
231 gnotobiotic zebrafish platform represents a disruptive technology that could be adapted to  
232 identify pathobiont species from human cardiovascular disease patients and as a “first pass”  
233 platform in mechanistic studies with appropriate zebrafish models of cardiovascular pathology.

234

235 Our investigation of *E. faecalis*-accelerated hyperlipidaemia uncovered a surprising role of Gram-  
236 positive cell wall component-triggered Myd88 signalling in zebrafish embryo lipid metabolism. The  
237 presence of this response in zebrafish embryos has broad implications for the use of zebrafish  
238 embryos to study transplanted mammalian microbiota as it may not be representative of the  
239 mammalian response to colonisation with Gram positive organisms. Most zebrafish embryo mono-  
240 association studies have been carried out with Gram negative organisms including *E. coli*, *A.*  
241 *veronii*, *V. cholerae*, and *P. aeruginosa* [17-19].

242

243 The comparison of heat killed *E. faecalis* to heat killed *S. xylosus* demonstrated an increased ability  
244 of heat killed *E. faecalis* to accelerate diet-induced hyperlipidaemia. This suggests that there is  
245 variability in hyperlipidaemia accelerating potential amongst Gram positive organisms in zebrafish  
246 embryos. The basis of this difference could be further explored using model Gram positive  
247 organisms and Gram-positive organisms that are natural commensals in the zebrafish gut. A recent

248 paper by Griffin *et al.* has demonstrated a role for *E. faecalis* SagA enzyme in producing immuno-  
249 stimulatory muropeptides [20], as we have previously demonstrated a conserved function of the  
250 zebrafish NOD orthologs it is possible that SagA-mediated production of muropeptides from  
251 bacterial peptidoglycan contributes to our hyperlipidaemia-accelerating phenotype.

252

253 *Caenorhabditis elegans* fed with *S. maltophilia* accumulate neutral lipids within intracellular lipid  
254 droplets driven by a bacterially-encoded mechanism that is independent of the innate immune  
255 response [21]. Our finding that two distinct mouse-associated *S. maltophilia* strains were able to  
256 increase the hyperlipidaemic potential of chicken egg yolk suggests the digestive ability of *S.*  
257 *maltophilia* is potentially conserved between strains and potentially between host species.  
258 Previous studies have identified *S. maltophilia* strains within zebrafish gut microbiomes [9], these  
259 zebrafish-associated strains could be analysed to determine if increased lipid uptake is a  
260 consequence of natural host-*S. maltophilia* pairs and for comparative studies to identify the food  
261 modifying mechanisms employed by our *S. maltophilia* CD103 strain isolate.

262

263 We also found an embryo growth-enhancing effect of pre-digesting commercially available  
264 zebrafish embryo feed with *S. maltophilia* which suggests *S. maltophilia* could have commercial  
265 applications as an aquaculture feed additive. The use of *S. maltophilia* as a feed additive is  
266 potentially risky as this organism is associated with opportunistic infections in humans and is  
267 resistant to a wide range of antibiotics so care should be taken to avoid cross over into the food  
268 chain [22, 23].

269

270 As a proof-of-principle study, our work demonstrates the feasibility of studying the interaction of  
271 bacterial species transplanted from a mammalian host with an environmental factor to result in a  
272 conditional phenotype in the tractable zebrafish model system. Further work is required to

273 examine effects of the two pathobiont species identified in our study on mammalian models of  
274 hyperlipidaemia and to correlate their colonisation with the progression of cardiovascular disease  
275 phenotypes in mammalian models and human samples.

276

277 **Methods**

278 Zebrafish handling

279 Adult zebrafish were housed at the Centenary Institute (Sydney Local Health District Animal  
280 Welfare Committee Approval 17-036). Zebrafish embryos were obtained by natural spawning and  
281 conventionally raised embryos were maintained in E3 media at 28°C.

282

283 Generation of microbiome-depleted (MD) zebrafish embryos

284 Microbiome-depleted (MD) zebrafish were created and maintained as previously described [24].  
285 Briefly, freshly laid embryos were rinsed with 0.003% v/v bleach in sterile E3 and rinsed 3 times  
286 with sterile E3. Bleached embryos were raised in sterile E3 supplemented with 50 µg/mL ampicillin  
287 (Sigma), 5 µg/mL kanamycin (Sigma) and 250 ng/mL amphotericin B (Sigma) in sterile tissue  
288 culture flasks. Dead embryos and chorions were aseptically removed at one and three dpf  
289 respectively.

290

291 Conventionalised zebrafish were used as a control, where 3 dpf MD zebrafish were inoculated  
292 with system water from the aquarium at Centenary Institute.

293

294 Generation of mouse faecal microbiota specimens

295 Mice were housed at the Centenary Institute (Sydney Local Health District Animal Welfare  
296 Committee Approval 2018/016). C57BL/6J mice were housed in a pathogen-free and temperature-  
297 controlled environment, with 12 hours of light and 12 hours of darkness, and free access to food

298 and water. Mice were provided with a High Fat Diet (HFD) or chow from 6 to 30 weeks of age. The  
299 HFD was prepared in-house based on rodent diet no. D12451 (Research Diets New Brunswick,  
300 USA) and its calories were supplied as: fat 45%, protein 20%, and carbohydrate 35% [25]. The  
301 chow diet was commercially produced by Speciality Feeds as “Irradiated Rat and Mouse Diet” and  
302 its calories were supplied as: fat 12%, protein 23%, and carbohydrate 65%.

303

304 Faecal pellets were collected from mice that were housed in different cages. Individual faecal  
305 pellets were collected into sterile 1.7 mL microcentrifuge tubes and homogenised in 1 mL of sterile  
306 E3 by pipetting. Homogenised specimens were centrifuged at 500 G for 2 minutes to sediment  
307 fibrous material and the supernatant was collected. Supernatants were supplemented with  
308 glycerol to a final concentration of 25% v/v, aliquoted, and frozen at -80°C for experimental use.

309

310 Colonisation of zebrafish with mouse faecal microbiota

311 MD zebrafish were colonised at 3 dpf by transfer into sterile E3 and addition of 200 µL thawed  
312 faecal homogenate supernatant. At 5 dpf, embryos were rinsed with E3 and placed on a chicken  
313 egg yolk diet.

314

315 Neutral red staining and morphology measurements

316 Neutral red staining was performed as previously described [26]. Briefly, 2.5 µg/mL neutral red  
317 was added to the media of 4 dpf embryos and incubated overnight. Embryos were rinsed with  
318 fresh E3 to remove unbound neutral red and live imaged on a Leica M205FA microscope with a  
319 consistent zoom between specimens in a single experiment. The area of neutral red-stained  
320 midgut was measured in pixels using ImageJ. Body size was measured in pixels using ImageJ.

321

322 Zebrafish high fat diet challenge with chicken egg yolk

323 High fat diet challenge with chicken egg yolk was performed as previously described [13]. Briefly, 5  
324 dpf zebrafish embryos were placed in an E3 solution containing 0.05% w/v emulsified hard boiled  
325 chicken egg yolk in glass beakers. Beakers were housed in a 28°C incubator with a 14:10 hour  
326 light:dark cycle. The emulsified hard boiled chicken egg yolk solution was changed daily.

327

328 Oil Red O staining assay

329 Oil Red O staining and analysis was performed as previously described [13, 27, 28]. Briefly, 7 dpf  
330 embryos were fixed overnight at 4°C in 4% paraformaldehyde, rinsed with PBS, and rinsed  
331 stepwise through to propylene glycol. Embryos were stained with filtered 0.5% (w/v) Oil Red O  
332 dissolved in propylene glycol overnight at room temperature. Unbound dye was removed by  
333 washing with propylene glycol and embryos were rinsed stepwise through to PBS for imaging.

334

335 Embryos were imaged on a Leica M205FA microscope. Experimental batches of colour images  
336 were analysed in ImageJ by adjusting the colour threshold function to eliminate non-red signal,  
337 this output was then converted to a binary mask and the tail region posterior to the swim bladder  
338 was selected to measure the area of particles.

339

340 Isolation, identification, and handling of bacterial isolates from mouse faecal microbiota samples

341 Faecal homogenate supernatants were plated onto LB Agar (Ampic Media) and incubated at 28°C  
342 for two days. Individual isolates were grown in broth culture in Luria Broth (Miller's LB Broth Base,  
343 Thermofisher) at 28°C overnight with 200 RPM shaking.

344

345 For identification, bacteria were harvested from broth culture and subjected to PCR using  
346 universal 16S primers (5'-3') Fw Rv. PCR products were sequenced by Sanger Sequencing (AGRF)

347 and NCBI records were searched by BLAST to identify the closest matching bacterial strain by  
348 sequence identity.

349

350 For gnotobiotic experiments, bacteria were harvested from overnight broth cultures and  
351 resuspended in sterile E3 zebrafish embryo media at a concentration of OD600 0.2. MD zebrafish  
352 in autoclaved E3 were then inoculated with the bacterial suspension at a ratio of 1:200.

353

354 For heat killed bacterial inoculations, bacteria were resuspended in E3 at a concentration of  
355 OD600 0.2 and heat-killed in a 95°C heat block for 30 minutes. Heat killed bacterial solutions were  
356 then added at 1:200 ratio to 3 dpf MD zebrafish.

357

358 For purified ligand exposure, 3 dpf MD zebrafish were soaked in 25 µg/mL lipoteichoic acid  
359 (Sigma) or 25 µg/mL peptidoglycan (Sigma).

360

361 For lysozyme digestion of heat-killed *E. faecalis*, a suspension of heat-killed bacteria was incubated  
362 with 50 µg/mL lysozyme (Sigma) at 37°C for 6 h before being used to inoculate 3 dpf MD zebrafish  
363 at a ratio of 1:200.

364

365 Digestion of chicken egg yolk

366 20 g hard-boiled chicken egg yolk was mixed with 40 mL E3 and emulsified using a Branson Digital  
367 Sonifier sonicator. Emulsified egg yolk was inoculated with bacterial isolates in E3 (described  
368 above) at a 1:200 ratio. Egg yolk mixture was then placed in a shaker at 28 °C at 200 rpm and for  
369 48 h. Samples were then autoclaved prior to feeding experiments.

370

371 Analysis of chicken egg yolk composition

372 “Pre-digested” samples were autoclaved and mailed to Australian Laboratory Services (VIC,  
373 Australia) for commercial grade nutritional analyses.

374

375 Gene knockdown with CRISPR-Cas9

376 gRNA templates for *myd88* (5`- 3`): Target 1

377 TAATACGACTCACTATAGGCAGTTCCGAAAGAAACTGTTTAGAGCTAGAAATAGC, Target 2

378 TAATACGACTCACTATAGGAAAAGGTCTGACGGACTGTTTAGAGCTAGAAATAGC, Target 3

379 TAATACGACTCACTATAGGAACGTGGATCATCTCGGTTTAGAGCTAGAAATAGC, Target 4

380 TAATACGACTCACTATAGGTTTCGATAAGCTACGTTTAGAGCTAGAAATAGC. gRNA was

381 synthesized as previously described [29].

382

383 A 1:1 solution of gRNA and 500 µg/mL of Cas9 nuclease V3 (Integrated DNA Technology, Sigma, or  
384 or Sydney Analytical) was prepared with phenol red dye (Sigma, P0290). Freshly laid eggs were  
385 collected from breeding tanks and the solution was injected in the yolk sac of the egg before the  
386 emergence of the first cell with a FemtoJet 4i (Eppendorf).

387

388 Knockdown efficacy was monitored by RT-qPCR as previously described [30]. *myd88*-specific  
389 primers (5`- 3`): Fw ACAGGGACTGACACCTGAGA, Rv GACGACAGGGATTAGCCGTT.

390

391 To derive MD crispant embryos, injected embryos were placed in E3 containing ampicillin,  
392 kanamycin and amphotericin B as described previously. Bleaching injected embryos caused high  
393 mortality rates.

394

395 Statistics

396 All statistical analyses (t-tests and ANOVA where appropriate) were performed using GraphPad  
397 Prism 8. Outliers were removed using ROUT, with Q = 1%. All data shown are representative of at  
398 least 2 biological replicates.

399

400 **Data availability**

401 Source data are provided with this paper.  
402 Raw image and analysis data is archived for 10 years by The Centenary Institute and available on  
403 request from the corresponding author (Sydney, Australia).

404

405 **Acknowledgements**

406 Funding: Australian National Health and Medical Research Council Project Grant APP1099912; The  
407 University of Sydney Fellowship G197581; NSW Ministry of Health under the NSW Health Early-  
408 Mid Career Fellowships Scheme H18/31086 to SHO. Australian National Health and Medical  
409 Research Council Centres of Research Excellence Grant APP1153493 to WJB. The funders had no  
410 role in study design, data collection and analysis, decision to publish, or preparation of the  
411 manuscript.

412

413 The *E. faecalis* UNSW 054400 type strain was provided by Dr Laurence Marcia.

414

415 The authors acknowledge the facilities and the technical assistance of Dr Angela Kurz at the  
416 BioImaging Facility and Sydney Cytometry at Centenary Institute, and Dr Mario Torrado Del Rey of  
417 Sydney Analytical at The University of Sydney for supply of some Cas9 protein.

418

419 The authors declare no conflicts of interest.

420

421 **References**

- 422 1. Sekirov, I., et al., *Gut microbiota in health and disease*. *Physiol Rev*, 2010. **90**(3): p. 859-904.
- 423 2. Backhed, F., et al., *Mechanisms underlying the resistance to diet-induced obesity in germ-free mice*. *Proc Natl Acad Sci U S A*, 2007. **104**(3): p. 979-84.
- 424 3. Arias-Jayo, N., et al., *High-Fat Diet Consumption Induces Microbiota Dysbiosis and Intestinal Inflammation in Zebrafish*. *Microb Ecol*, 2018. **76**(4): p. 1089-1101.
- 425 4. Rawls, J.F., et al., *Reciprocal gut microbiota transplants from zebrafish and mice to germ-free recipients reveal host habitat selection*. *Cell*, 2006. **127**(2): p. 423-33.
- 426 5. Murphy, E.A., K.T. Velazquez, and K.M. Herbert, *Influence of high-fat diet on gut microbiota: a driving force for chronic disease risk*. *Curr Opin Clin Nutr Metab Care*, 2015. **18**(5): p. 515-20.
- 427 6. Ridaura, V.K., et al., *Gut microbiota from twins discordant for obesity modulate metabolism in mice*. *Science*, 2013. **341**(6150): p. 1241214.
- 428 7. Lopez Nadal, A., et al., *Feed, Microbiota, and Gut Immunity: Using the Zebrafish Model to Understand Fish Health*. *Front Immunol*, 2020. **11**: p. 114.
- 429 8. Brinkmann, B.W., et al., *Colonizing microbiota protect zebrafish larvae against silver nanoparticle toxicity*. *Nanotoxicology*, 2020. **14**(6): p. 725-739.
- 430 9. Stressmann, F.A., et al., *Mining zebrafish microbiota reveals key community-level resistance against fish pathogen infection*. *ISME J*, 2021. **15**(3): p. 702-719.
- 431 10. Valenzuela, M.J., et al., *Evaluating the Capacity of Human Gut Microorganisms to Colonize the Zebrafish Larvae (*Danio rerio*)*. *Front Microbiol*, 2018. **9**: p. 1032.
- 432 11. Bates, J.M., et al., *Distinct signals from the microbiota promote different aspects of zebrafish gut differentiation*. *Dev Biol*, 2006. **297**(2): p. 374-86.
- 433 12. Oehlers, S.H., et al., *A chemical enterocolitis model in zebrafish larvae that is dependent on microbiota and responsive to pharmacological agents*. *Dev Dyn*, 2011. **240**(1): p. 288-98.
- 434 13. Morris, S., et al., *Glucose inhibits haemostasis and accelerates diet-induced hyperlipidaemia in zebrafish larvae*. *Sci Rep*, 2021.
- 435 14. Cheesman, S.E., et al., *Epithelial cell proliferation in the developing zebrafish intestine is regulated by the Wnt pathway and microbial signaling via Myd88*. *Proc Natl Acad Sci U S A*, 2011. **108 Suppl 1**: p. 4570-7.
- 436 15. Novoa, B., et al., *LPS response and tolerance in the zebrafish (*Danio rerio*)*. *Fish Shellfish Immunol*, 2009. **26**(2): p. 326-31.
- 437 16. Kaye, D.M., et al., *Deficiency of Prebiotic Fiber and Insufficient Signaling Through Gut Metabolite-Sensing Receptors Leads to Cardiovascular Disease*. *Circulation*, 2020. **141**(17): p. 1393-1403.
- 438 17. Tan, F., et al., *The Responses of Germ-Free Zebrafish (*Danio rerio*) to Varying Bacterial Concentrations, Colonization Time Points, and Exposure Duration*. *Front Microbiol*, 2019. **10**: p. 2156.
- 439 18. Weitekamp, C.A., et al., *Monoassociation with bacterial isolates reveals the role of colonization, community complexity and abundance on locomotor behavior in larval zebrafish*. *Anim Microbiome*, 2021. **3**(1): p. 12.
- 440 19. Robinson, C.D., et al., *Experimental bacterial adaptation to the zebrafish gut reveals a primary role for immigration*. *PLoS Biol*, 2018. **16**(12): p. e2006893.
- 441 20. Griffin, M.E., et al., *Enterococcus peptidoglycan remodeling promotes checkpoint inhibitor cancer immunotherapy*. *Science*, 2021. **373**(6558): p. 1040-1046.
- 442 21. Xie, K., et al., *Dietary *S. maltophilia* promotes fat storage by enhancing lipogenesis and ER-LD contacts in *C. elegans**. *bioRxiv*, 2020: p. 2020.04.29.067793.

469 22. Brooke, J.S., *Stenotrophomonas maltophilia: an emerging global opportunistic pathogen*.  
470 *Clin Microbiol Rev*, 2012. **25**(1): p. 2-41.

471 23. Pathmanathan, A. and G.W. Waterer, *Significance of positive Stenotrophomonas*  
472 *maltophilia culture in acute respiratory tract infection*. *Eur Respir J*, 2005. **25**(5): p. 911-4.

473 24. Melancon, E., et al., *Best practices for germ-free derivation and gnotobiotic zebrafish*  
474 *husbandry*. *Methods Cell Biol*, 2017. **138**: p. 61-100.

475 25. Henderson, J.M., et al., *Multiple liver insults synergize to accelerate experimental*  
476 *hepatocellular carcinoma*. *Sci Rep*, 2018. **8**(1): p. 10283.

477 26. Oehlers, S.H., et al., *Chemically induced intestinal damage models in zebrafish larvae*.  
478 *Zebrafish*, 2013. **10**(2): p. 184-93.

479 27. Fang, L., et al., *In vivo visualization and attenuation of oxidized lipid accumulation in*  
480 *hypercholesterolemic zebrafish*. *J Clin Invest*, 2011.

481 28. Johansen, M.D., et al., *Mycobacterium marinum infection drives foam cell differentiation in*  
482 *zebrafish infection models*. *Dev Comp Immunol*, 2018. **88**: p. 169-172.

483 29. Wu, R.S., et al., *A Rapid Method for Directed Gene Knockout for Screening in GO Zebrafish*.  
484 *Dev Cell*, 2018. **46**(1): p. 112-125 e4.

485 30. Cholan, P.M., et al., *Conserved anti-inflammatory effects and sensing of butyrate in*  
486 *zebrafish*. *Gut Microbes*, 2020. **12**(1): p. 1-11.

487

488 **Figure Legends**

489 Figure 1: Transplantation of microbiota from HFD-fed mice accelerates hyperlipidaemia in  
490 zebrafish embryos.

491 (a) Schematic describing method of faecal microbiome inoculation in MD zebrafish and chicken  
492 egg yolk challenge diet. (b) Representative images of neutral red staining in mid-gut of 5 dpf  
493 zebrafish embryos. Red brackets indicate mid-gut region used for quantification. (c) Quantification  
494 of neutral red staining area in mid-gut of 5 dpf zebrafish embryos. (d) Representative images of Oil  
495 Red O staining of 7 dpf chow-fed and HFD-fed mouse faecal microbiome-inoculated zebrafish  
496 embryos. Red brackets indicate tail region posterior to the swim bladder used for quantification  
497 (e) Quantification of trunk vascular Oil Red O staining from the tail region posterior to the swim  
498 bladder in MD zebrafish inoculated with mouse faecal microbiota and challenged with chicken egg  
499 yolk diet from 5-7 dpf. Scale bar represents 500  $\mu$ m. Results are expressed as mean  $\pm$  SD.

500

501 Figure 2: Identification of individual microbes with pathobiont activity.

502 (a) Schematic describing workflow to isolate *Escherichia species* PYCC8248 (*E.s*), *Escherichia coli*  
503 strain Y15 (*E.c*), and *Enterococcus faecalis* strain YN771 (*E.f*) and inoculate into MD zebrafish with  
504 subsequent chicken egg yolk diet challenge. (b) Quantification of trunk vascular Oil Red O staining  
505 from the tail region posterior to the swim bladder in MD zebrafish inoculated with bacterial  
506 isolates *E.s*, *E.c*, and *E.f* and challenged with a chicken egg yolk diet from 5-6 dpf. (c) Area of  
507 neutral red stained in the mid-gut of 5 dpf gnotobiotic zebrafish embryos mono-associated with  
508 bacterial isolates *E.s*, *E.c*, and *E.f*. (d) Quantification of trunk vascular Oil Red O staining from the  
509 tail region posterior to the swim bladder in MD zebrafish inoculated with bacterial isolates *E.f* and  
510 *E. faecalis* UNSW 054400 type strain (*E.f* UNSW) then challenged with a chicken egg yolk diet from  
511 5-6 dpf. Results are expressed as mean  $\pm$  SD.

512

513 Figure 3: *Stenotrophomonas maltophilia* accelerates hyperlipidaemia by digesting food.  
514 (a) Schematic describing creation of “pre-digested” chicken egg yolk by incubation with bacterial  
515 isolates *E.s*, *E.c*, *S.m*, and *E.f*, autoclaving, for feeding to 5-7 dpf zebrafish embryos. (b)  
516 Quantification of trunk vascular Oil Red O staining from the tail region posterior to the swim  
517 bladder in MD zebrafish fed “pre-digested” egg yolk with bacterial isolates *E.s*, *E.c*, *S.m*, and *E.f*  
518 from 5-7 dpf. (c) Quantification of trunk vascular Oil Red O staining from the tail region posterior  
519 to the swim bladder in conventionally raised zebrafish fed “pre-digested” egg yolk with bacterial  
520 isolate *S.m* from 5-7 dpf. (d) Quantification of trunk vascular Oil Red O staining from the tail region  
521 posterior to the swim bladder in conventionally raised zebrafish fed “pre-digested” fish embryo  
522 food with bacterial isolates *E.c* and *S.m* from 5-7 dpf. (e) Representative images of “pre-digested”  
523 egg yolk with bacterial isolates *E.c* and *S.m* red brackets indicate fraction of the water column  
524 containing large particulates after autoclaving. (f) CFU recovery from chicken egg yolk “pre-  
525 digestion” reactions. Results are expressed as mean  $\pm$  SD.

526

527 Figure 4: *Enterococcus faecalis* (*E.f*) accelerates hyperlipidaemia via host MyD88-mediated  
528 signalling.

529 (a) Schematic describing inoculation of MD zebrafish embryos with heat-killed bacterial isolates  
530 *E.s*, *E.c*, and *E.f* from 3-5 dpf, followed by chicken egg yolk diet challenge from 5-7 dpf. (b)  
531 Quantification of trunk vascular Oil Red O staining from the tail region posterior to the swim  
532 bladder in MD zebrafish inoculated with heat killed bacterial isolates *E.s*, *E.c*, and *E.f* and  
533 challenged with a chicken egg yolk diet. (c) Quantification of *myd88* expression in zebrafish  
534 embryos injected with *myd88*-targeting CRISPR-Cas9 complexes at 5 dpf. Each dot represents a  
535 biological replicate of at least 10 embryos. (d) Quantification of trunk vascular Oil Red O staining  
536 from the tail region posterior to the swim bladder in control scrambled and *myd88* crispant  
537 embryos exposed to *E.f* and challenged with a chicken egg yolk diet. Results are expressed as  
538 mean  $\pm$  SD.

539

540 Figure 5: Gram-positive cell wall components accelerate hyperlipidaemia in zebrafish embryos.

541 (a) Quantification of trunk vascular Oil Red O staining from the tail region posterior to the swim  
542 bladder in MD zebrafish inoculated with heat killed bacterial isolates *E.f* and *Staphylococcus*  
543 *xylosus* (*S.x*) from 3-5 dpf and challenged with a chicken egg yolk diet from 5-7 dpf. (b)  
544 Quantification of trunk vascular Oil Red O staining from the tail region posterior to the swim  
545 bladder in MD zebrafish pre-incubated with LTA or peptidoglycan from 3-5 dpf before co-  
546 challenge with chicken egg yolk diet from 5-7 dpf. (c) Quantification of trunk vascular Oil Red O  
547 staining from the tail region posterior to the swim bladder in MD zebrafish pre-incubated with  
548 lysozyme-treated heat killed *E.f* from 3-5 dpf and challenged with a chicken egg yolk diet from 5-7  
549 dpf. (d) Quantification of trunk vascular Oil Red O staining from the tail region posterior to the  
550 swim bladder in control scrambled and *myd88* crispant embryos pre-incubated with LTA or

551 peptidoglycan from 3-5 dpf before co-challenge with chicken egg yolk diet from 5-7 dpf. Results  
552 are expressed as mean  $\pm$  SD.  
553

# A Chow-fed mice

bioRxiv preprint doi: <https://doi.org/10.1101/2021.04.28.441900>; this version posted September 21, 2021. The copyright holder for this preprint (which was not certified by peer review) is the author/funder, who has granted bioRxiv a license to display the preprint in perpetuity. It is made available under aCC-BY-NC-ND 4.0 International license.



# HFD-fed mice



# MD zebrafish

0 dpf

3 dpf

# Inoculation period

5 dpf

7 dpf

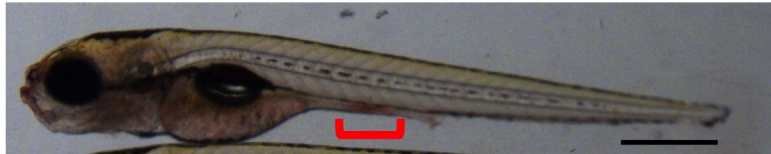


# Egg yolk

## B

### Neutral red staining

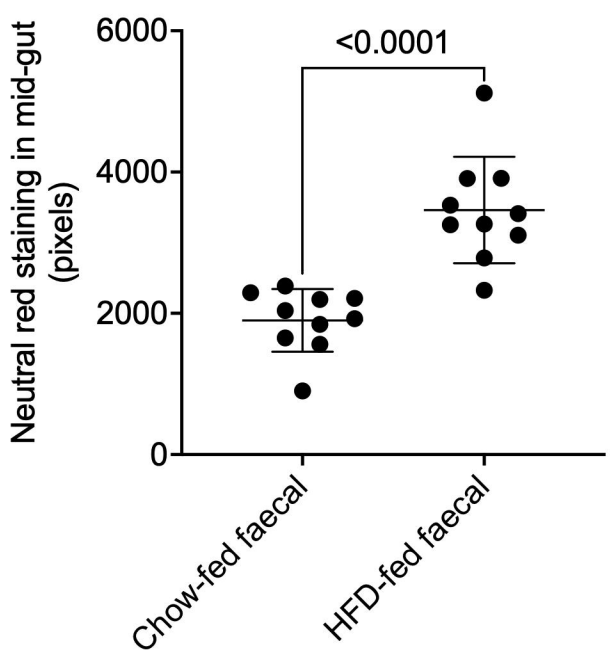
Chow-fed mouse faecal microbiome inoculated zebrafish



HFD-fed mouse faecal microbiome inoculated zebrafish



## C



## D

### Oil Red O staining

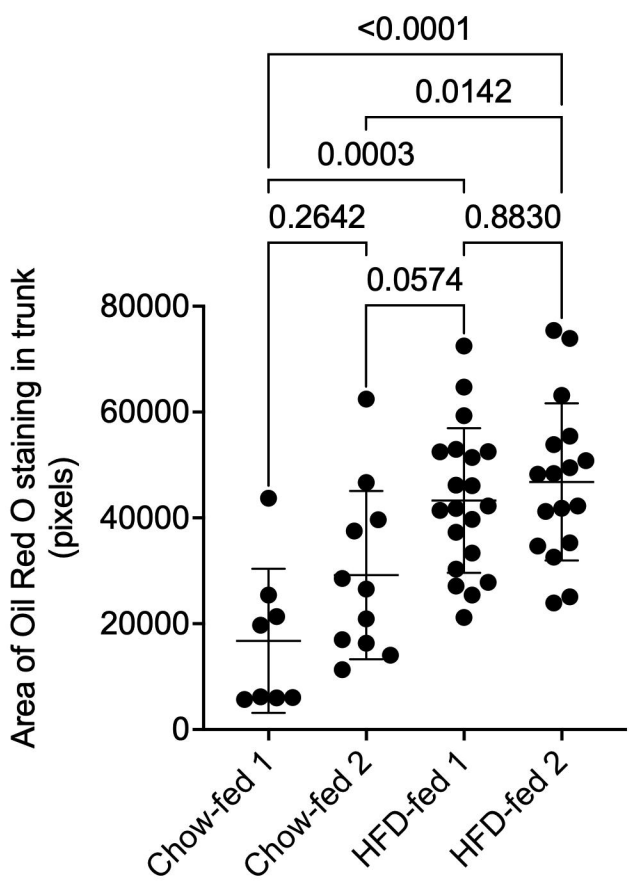
Chow-fed mouse faecal microbiome inoculated zebrafish

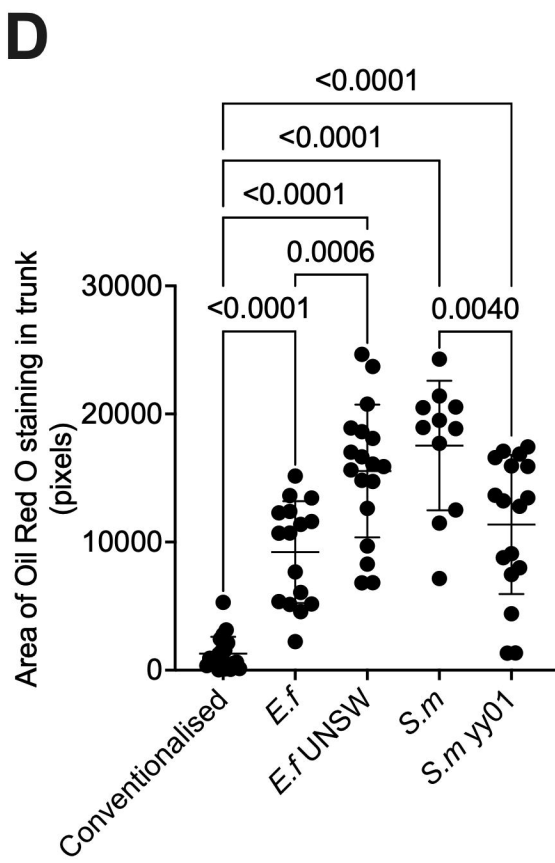
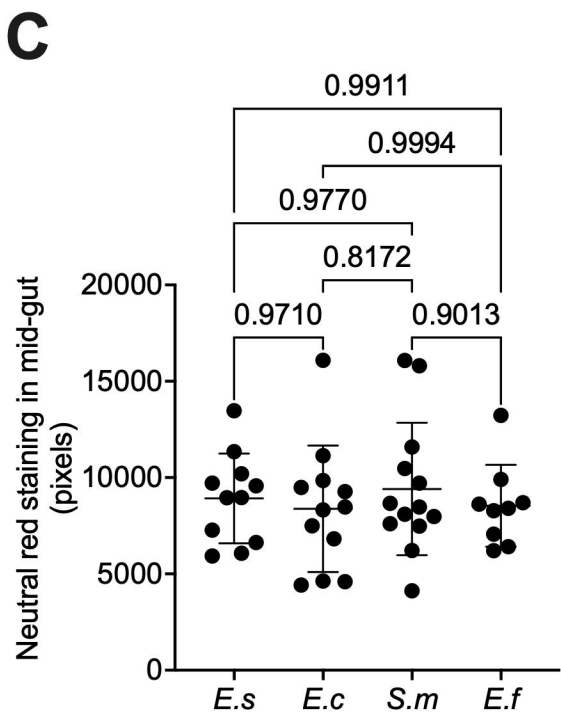
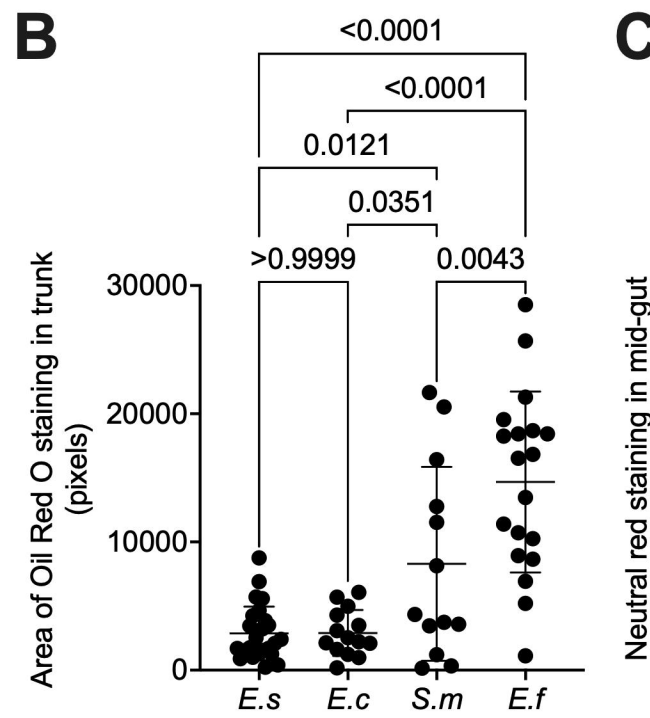
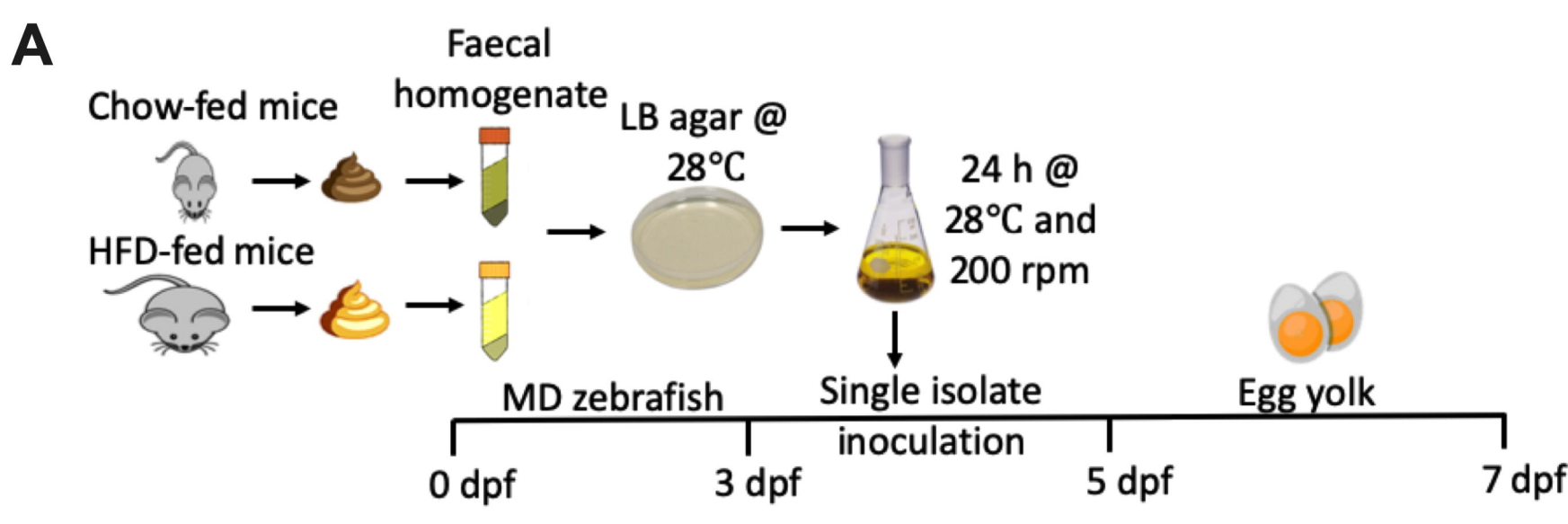


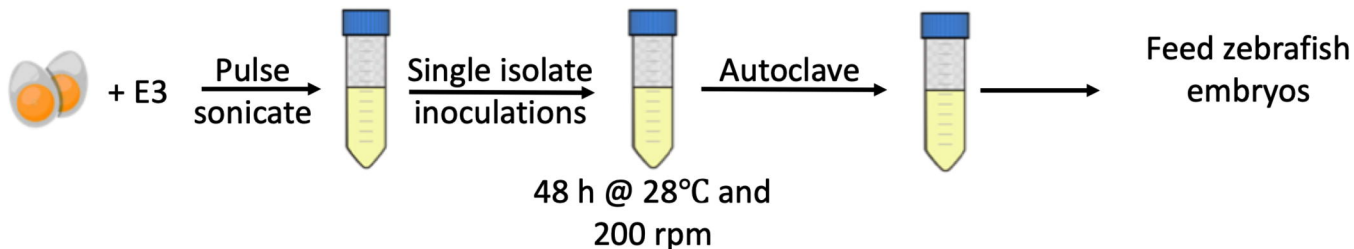
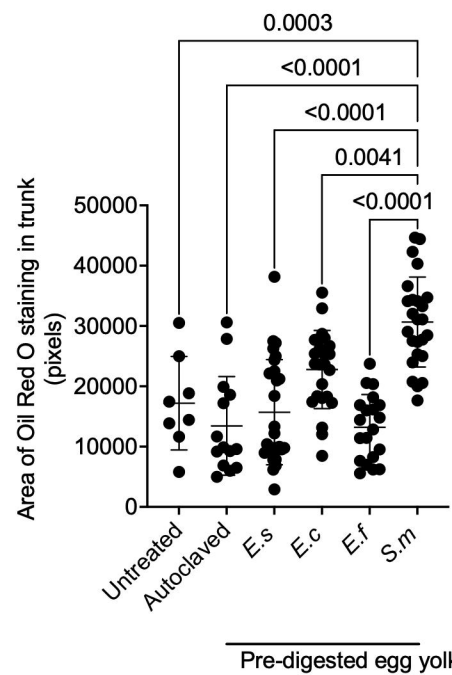
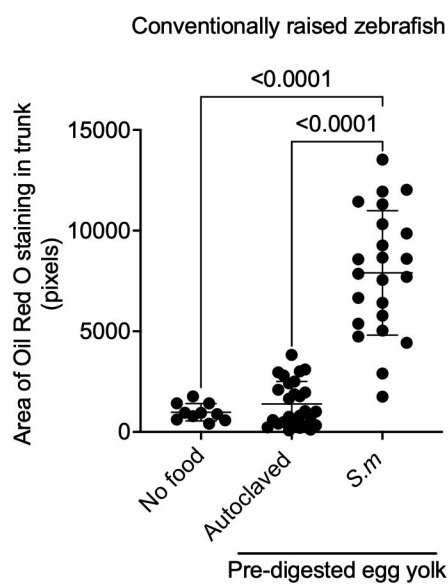
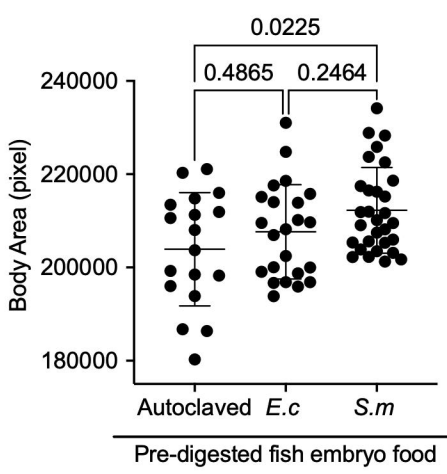
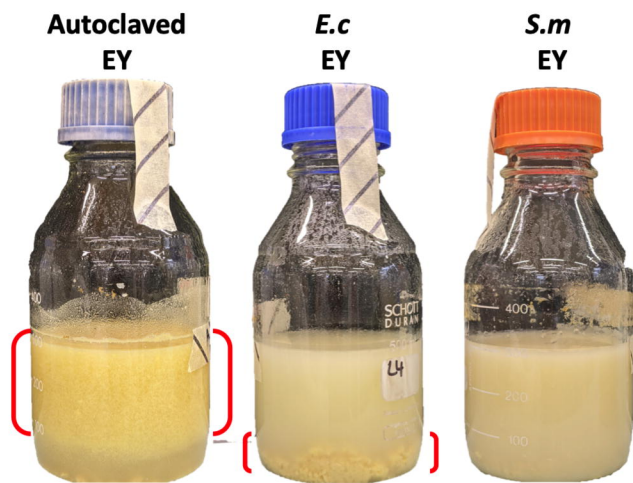
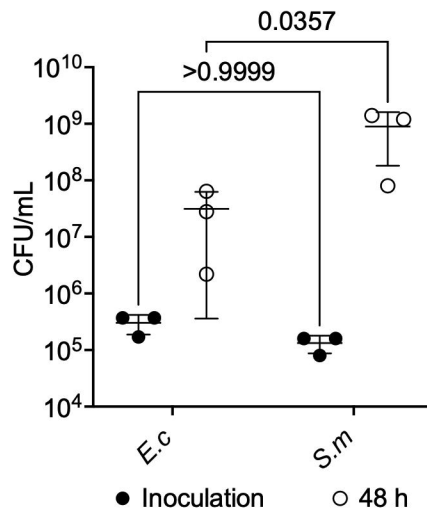
HFD-fed mouse faecal microbiome inoculated zebrafish

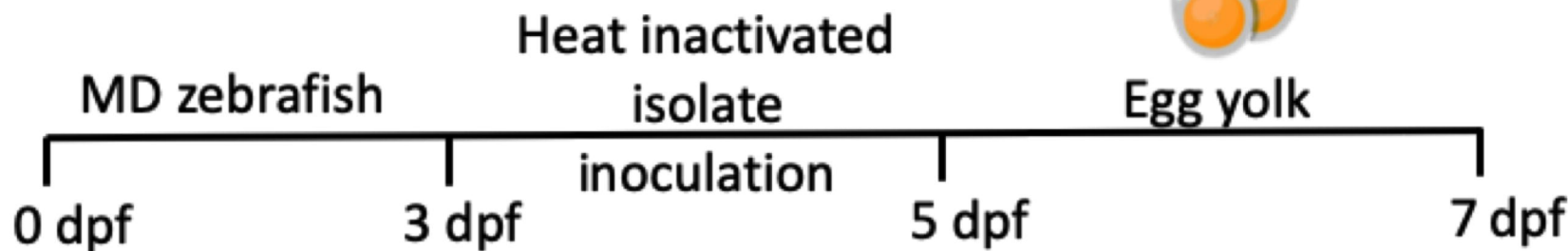
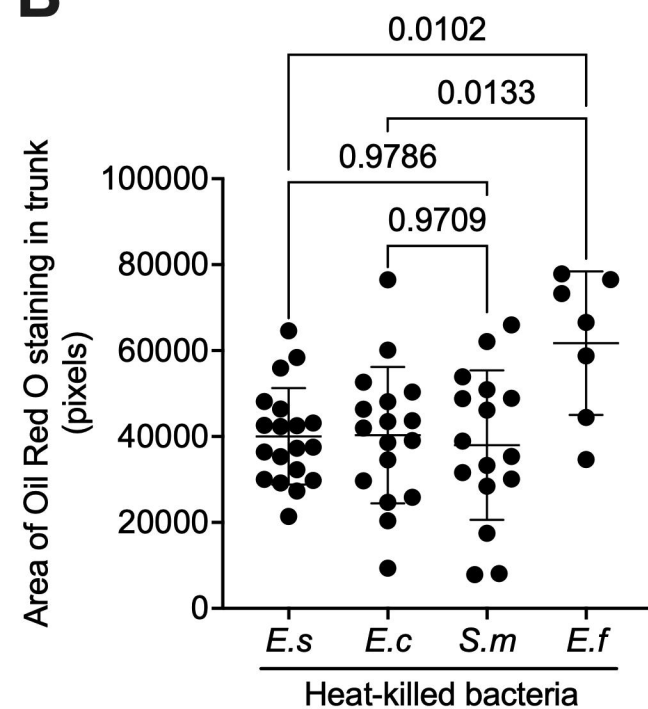
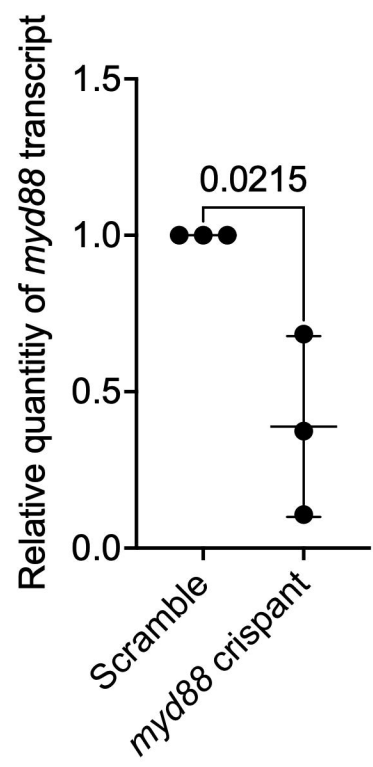
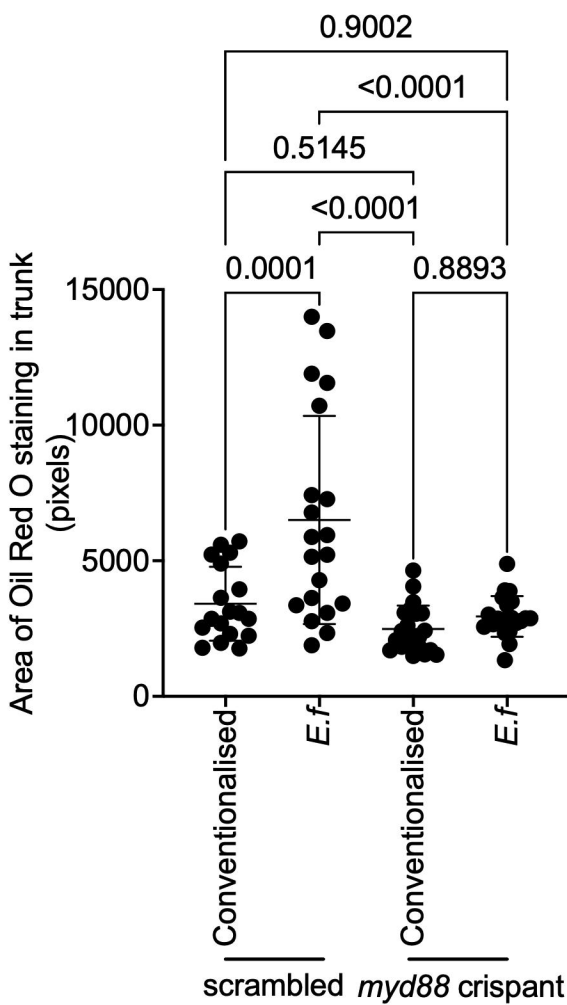


## E





**A****B****C****D****E****F**

**A****B****C****D**

scrambled      *myd88* crispant

